A Passive Repression Mechanism that Hinders Synergic Transcriptional Activation by Heat Shock Factors Involved in Sunflower Seed Longevity

Dear Editor,

Different genetic programs that are active during late stages of zygotic embryogenesis are involved in seed phenotypes as longevity, basal thermotolerance, and desiccation tolerance. In sunflower, Heat Shock Factor A9 (HaHSFA9) controls one of such programs, the HaHSFA9 program. Over-expression of HaHSFA9 in seeds of transgenic tobacco showed the involvement of this transcription factor in basal thermotolerance and longevity; HaHSFA9 activated a genetic program that includes specific small Heat Shock Protein (*sHSP*) genes, which are expressed mainly (or exclusively) during zygotic embryogenesis in seeds (Prieto-Dapena et al., 2006). We also used an active-repressor dominant-negative (DN) form of HaHSFA9, and thus we obtained a substantial reduction of both the accumulation of specific sHSPs and of seed longevity (Tejedor-Cano et al., 2010). In contrast, transcription-inactive DN forms were inefficient. We therefore inferred the participation of additional HSF(s) in controlling the genetic program activated by HaHSFA9, rather than involvement of a single master control HSF (i.e., HaHSFA9 only). These additional HSF(s) would belong to class A, as HaHSFA9 (Tejedor-Cano et al., 2010). Furthermore, we obtained a similar reduction of seed longevity upon the overexpression of stabilized forms of HaIAA27, an Aux/IAA protein that represses HaHSFA9 in sunflower embryos. That observation connected plant seed longevity with auxin hormone action and lead us to predicting that the additional HSF(s) involved in the activation of the HaHSFA9 program should be also repressed by HaIAA27 (Carranco et al., 2010). Here, we identify HaHSFA4a as one of these additional HSFs. We demonstrate a transcriptional synergism between HaHSFA4a and HaHSFA9. Furthermore, we provide evidence for a, novel, passive repression mechanism of this synergism by HaIAA27.

We used an immature-embryo sunflower cDNA library, and a yeast two-hybrid strategy using an inactive form of HaHSFA9 as the bait, to clone a HSF expressed in immature seeds. The cloned HSF was named HaHSFA4a, as it

clearly belongs to the A4a group of plant HSFs (Scharf et al., 2012). The complete protein encoded by the HaHSFA4a cDNA (Supplementary Figure S1) could substitute the yeast sole HSF in functional complementation assays. In addition, a $GAL4_{DBD}$-HaHSFA4a fusion protein activated transcription in yeast one-hybrid experiments (Supplementary Figure S2). Thus, HaHSFA4a is a transcriptional activator HSF that is functional in yeast.

We determined the domains of HaHSFA9 involved in two-hybrid interaction with HaHSFA4a. The oligomerization domain (OD) appears to be important; neither the DNA binding domain nor the C-terminal activation domain of HaHSFA9 are required for two-hybrid interaction (Supplementary Figure S3). We also confirmed *in vitro* a direct physical interaction between HaHSFA9 and HaHSFA4a by means of GST pull-down (Supplementary Figure S4). Using BiFC assays, we found that the interaction between HaHSFA4a and HaHSFA9 indeed occurs in plant nuclei (Figure 1H and Supplementary Figure S4). This result indicates that HaHSFA4a might help HaHSFA9 in the transcriptional activation of *sHSP* gene promoters in the HSFA9 seed genetic program. The results in Figure 1F and 1J show that HaHSFA9 and HaHSFA4a synergistically activate the *Hahsp17.7 G4* (G4) promoter in bombarded sunflower embryos and leaves (statistical analyses in Supplementary Table S1).

We investigated whether the nuclear localized HaHSFA9 (Supplementary Figure S4 and S5) could impair the nuclear export of HaHSFA4a. A HaHSFA4a:GFP fusion was localized mostly in the cytosol in leaves of *Nicotiana benthamiana* (Figure 1A). In contrast, co-expression of HaHSFA4a:GFP with HaHSFA9 caused a substantial increase of the nuclear localization of the former at the expense of a drastic reduction of the GFP signal in the cytosol (Figure 1C). This effect was similar to but not as strong as the localization change of HaHSFA4a caused by mutation of a nuclear export sequence (NES motif) present in HaHSFA4a (compare Figure 1B and 1C). Therefore, the interaction between HaHSFA9 and HaHSFA4a causes nuclear retention of HaHSFA4a. We also found that the sequences of HaHSFA9 that include the OD are required both for the nuclear retention of HaHSFA4a and for the synergism between HaHSFA4a and HaHSFA9. LpHSFA2, HaHSFA9, and two A2:A9 hybrid HSFs ($A2:A9_1$ and $A2:A9_2$) were tested. The nuclear retention

and the synergistic effect were not observed with LpHSFA2 or with the A2:$A9_1$ hybrid HSF, which lack the OD of HaHSFA9. In contrast, HaHSFA9 and the A2:$A9_2$ hybrid HSF (containing the HaHSFA9 OD) could synergize with HaHSFA4a and caused nuclear retention of HaHSFA4a (Figure 1C-E and F, Supplementary Table S1). Therefore, nuclear retention of HaHSFA4a by HaHSFA9 might contribute to their synergistic co-activation. This is similar to what demonstrated for the synergism of LpHSFA2 and LpHSFA1 in tomato (Chan-Schaminet et al., 2009).

The results in Figure 1G demonstrate BiFC interaction between the HaIAA27 protein and HaHSFA4a in bombarded immature embryos of sunflower. The interaction between HaIAA27 and HaHSFA4a occurred both in the cytosol and in the nucleus. The hetero-oligomerization of HSFs (Chan-Schaminet et al., 2009; Scharf et al., 2012) and the interaction of HaIAA27 with HaHSFA9 (Carranco et al., 2010) both involve the HSF OD. Thus, a possible effect of HaIAA27 would be that it impairs the interaction between HaHSFA9 and HaHSFA4a. Such possibility was analyzed by testing in bombarded sunflower embryos the effect of a stabilized form of HaIAA27 (HaIAA27mIIab, Carranco et al., 2010) on the BiFC interaction between HaHSFA9 and HaHSFA4a. Indeed, when the HaIAA27mIIab form was co-bombarded with HaHSFA4a and HaHSFA9, the nuclear interaction between the two HSFs was substantially reduced (compare Figure 1H and 1I).

That HaIAA27 represses the synergistic co-activation by HaHSFA9 and HaHSFA4a was observed in immature sunflower embryos. A very strong synergistic effect between HaHSFA9 and HaHSFA4a was observed (Figure 1J, see also Supplementary Table S1). This synergistic co-activation was fully abolished by HaIAA27. Indeed, in presence of HaIAA27, HaHSFA9 and HaHSFA4a activated the G4 promoter to the same levels as observed with only HaHSFA9 in absence of the repressor. Such drastic effect contrasted with the much moderate reduction of the transcriptional activation by either HaHSFA9 or HaHSFA4a when the effect of HaIAA27 was analyzed in separate (Figure 1J).

The results in Figure 1H-J indicate that HaIAA27 might repress the synergism mainly by a passive mechanism. Active repression of Auxin

Response Factors (ARFs) by Aux/IAA proteins strictly depend on conserved leucine residues within domain I that are involved in interaction with TPL co-repressors (Tiwari et al., 2004; Szemenyei et al., 2008). We analyzed if domain I mutant forms of HaIAA27 where these leucines are substituted by alanine still repress the HaHSFA9/A4a synergism. In HaIAA27mIa the L19, L21 and L23 residues within domain I were substituted. In HaIAA27mIab two additional leucine residues (L12 and L14) were substituted. Both the mIa and mIab mutants repressed the synergism in a similar way as the WT HaIAA27 protein (Figure 1J). The similar repression of the synergism by the WT, mIa, and mIab proteins contrasts with a clear reduction of repression of 35S-induced transcription observed with both mIa and mIab when compared to the WT HaIAA27 (Figure 1K). The reduction of active repression by these mutant proteins would thus not affect repression of the HaHSFA9/A4a synergism. We conclude that the HaIAA27 WT protein, which is stabilized in the immature embryos employed in Figure 1G-K (Carranco et al., 2010), does not require the conserved leucines of domain I for repressing the HaHSFA9/A4a synergism. Thus, the observed repression would mainly occur by means of a novel passive mechanism. This agrees with previously published results from our lab that remained so far unexplained. Thus, the overexpression of either HaIAA27 or HaIAA27ΔN, a stabilized form of HaIAA27 that lacks N-terminal sequences including domains I and II caused similar effects in transgenic tobacco. In both cases, loss of function of the HaHSFA9 program was observed, leading to reduction of seed longevity (Carranco et al., 2010). However, HaIAA27ΔN does not appear to contain unmapped active repression domains; HaIAA27ΔN, as the mIa and mIab proteins did not efficiently repress 35S-induced transcription (Figure 1K). This is consistent with the expected localization of active repression domains in Aux/IAA proteins: usually within domain I, and in some cases between domains I and II (Tiwari et al., 2004; Li et al., 2011). Because auxin induces the destabilization of HaIAA27 (Carranco et al., 2010), we propose that auxin might relieve the, HaIAA27-mediated, repression of the synergism between HaHSFA9 and HaHSFA4a; this would lead to the transcriptional activation of the genetic program of seed longevity controlled by at least these two HSFs. The total number of involved HSFs in sunflower is still

unknown and it might differ between different plants. It is tempting to speculate that some natural Aux/IAA proteins, which as HaIAA27ΔN are devoid of domains I and II, in plants as for example poplar and maize (Kalluri et al., 2007; Wang et al., 2010), may still be able to modulate auxin responses through passive repression mechanisms similar to what we reported here.

SUPPLEMENTARY DATA

Supplementary Data are included.

FUNDING

This work was supported by the European Regional Development Fund (FEDER) and the Spanish Secretary of Research, Development, and Innovation (Grants BIO2008-00634 and BIO2011-23440 to JJ). Additional funds were obtained from the Andalusian Regional Government (Grant BIO148 to JJ).

ACKNOWLEDGEMENTS

We thank Dieter Scharf and Lutz Nover for manuscript pre-evaluation and advice. We also thank Masaru Ohme-Takagi, and Pierre Forbert for the reporter plasmid and GAL4DB parent plasmids used for the repression assays of Figure 1K. We are indebted to Francisco Javier Durán for his assistance with plant material.

Javier Tejedor-Cano[2], Raúl Carranco[2], José-María Personat, Pilar Prieto-Dapena, Concepción Almoguera, José Manuel Espinosa, and Juan Jordano[1]

Departamento de Biotecnología Vegetal, Instituto de Recursos Naturales y Agrobiología de Sevilla. Consejo Superior de Investigaciones Científicas (CSIC). Seville, Spain.

[1]To whom correspondence should be addressed. Email: juan.jordano@csic.es, Tel. +34 954 624711 (ext. 145), Fax +34 954 624002

[2]Equally contributing authors

REFERENCES

Carranco, R., Espinosa, J.M., Prieto-Dapena, P., Almoguera, C., and Jordano, J. (2010). Repression by an auxin/indole acetic acid protein connects auxin signaling with heat shock factor-mediated seed longevity. Proc. Natl. Acad. Sci. USA. **107,** 21908-21913.

Chan-Schaminet, K.Y., Baniwal, S.K., Bublak, D., Nover, L., and Scharf, K.D. (2009). Specific interaction between tomato HsfA1 and HsfA2 creates hetero-oligomeric superactivator complexes for synergistic activation of heat stress gene expression. J. Biol. Chem. **284,** 20848-20857.

Kalluri, U.C., Difazio, S.P., Brunner, A.M., and Tuskan, G.A. (2007). Genome-wide analysis of Aux/IAA and ARF gene families in *Populus trichocarpa*. BMC Plant Biol. **7,** 59.

Li, H., Tiwari, S.B., Hagen, G., and Guilfoyle, T.J. (2011). Identical amino acid substitutions in the repression domain of auxin/indole-3-acetic acid proteins have contrasting effects on auxin signaling. Plant Physiol. **155,** 1252-1263.

Prieto-Dapena, P., Castaño, R., Almoguera, C., and Jordano, J. (2006). Improved resistance to controlled deterioration in transgenic seeds. Plant Physiol. **142,** 1102-1112.

Scharf, K.D., Berberich, T., Ebersberger, I., and Nover L. (2012). The plant heat stress transcription factor (Hsf) family: Structure, function and evolution. Biochim. Biophys. Acta. **1819,** 104-119.

Szemenyei, H., Hannon, M., and Long, J.A. (2008). TOPLESS mediates auxin-dependent transcriptional repression during Arabidopsis embryogenesis. Science. **319,** 1384-1386.

Tejedor-Cano, J., Prieto-Dapena, P., Almoguera, C., Carranco, R., Hiratsu, K., Ohme-Takagi, M., and Jordano J. (2010). Loss of function of the HSFA9 seed longevity program. Plant Cell Environ. **33,** 1408-1417.

Tiwari, S.B., Hagen, G., and Guilfoyle, T.J. (2004). Aux/IAA proteins contain a potent transcriptional repression domain. Plant Cell. **16,** 533-543.

Wang, Y., Deng, D., Bian, Y., Lv Y., and Xie, Q. (2010). Genome-wide analysis of primary auxin-responsive Aux/IAA gene family in maize (*Zea mays*. L.). Mol. Biol. Rep. **37,** 3991-4001.

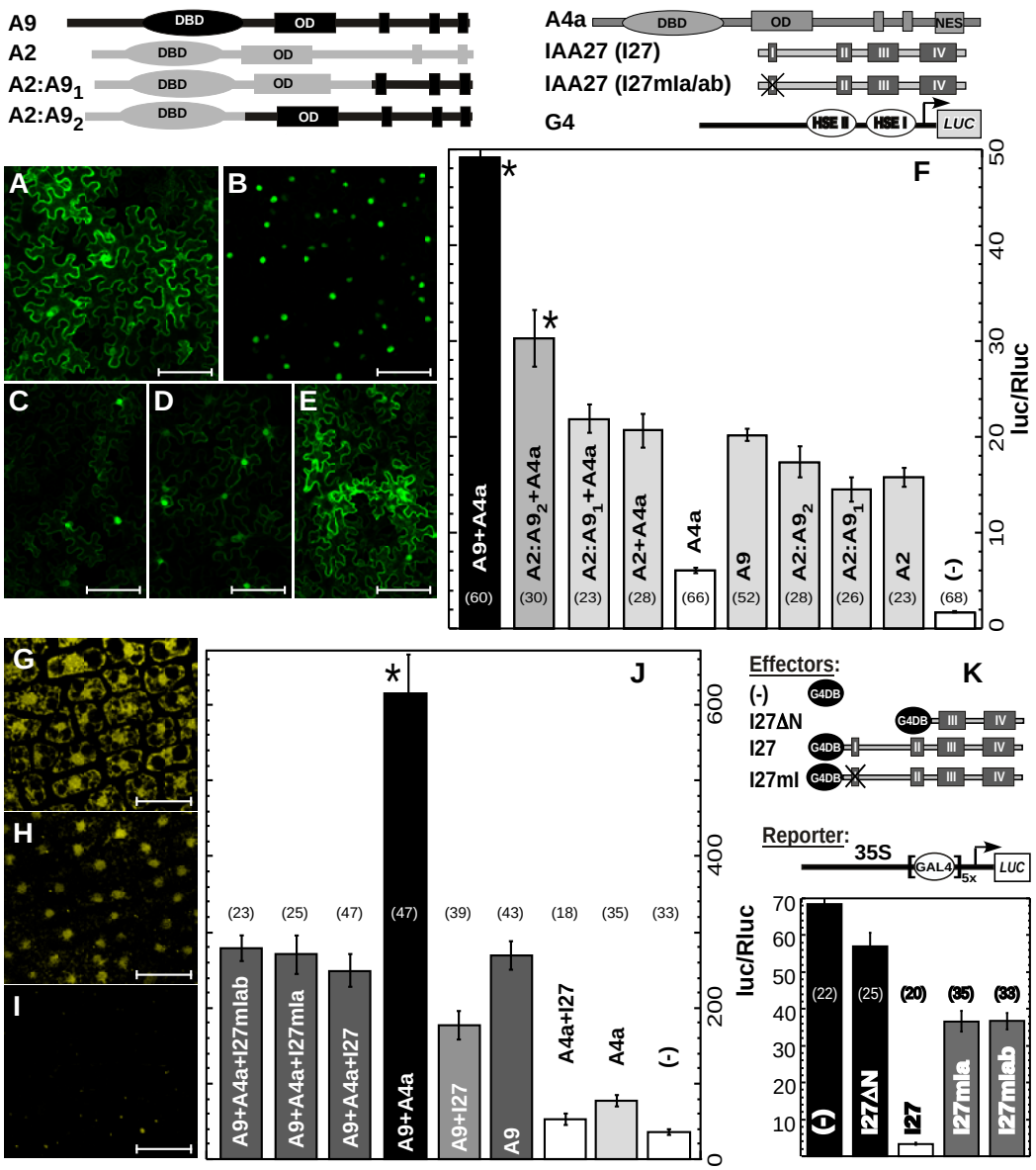

Figure 1. Passive repression by HaIAA27 of the synergism between HaHSFA9 and HaHSFA4a.

(A, B) Mostly cytosolic localization of HaHSFA4a:GFP (A) and enhanced nuclear localization of the NES mutant protein HaHSFA4a(NESmut):GFP (B).
(C, D, E) Co-expression of HaHSFA4a:GFP with HaHSFA9 (C), or with the hybrid HSF A2:A9$_2$ (D), but not with the hybrid HSF A2:A9$_1$ (E) enhanced nuclear localization of HaHSFA4a:GFP. Assays performed in leaves of *Nicotiana benthamiana*. Bars 100 µm.
(F) A synergistic transcriptional activation with HaHSFA4a (A4a) was observed using HaHSFA9 (A4a+A9), or with A2:A9$_2$ (A4a+A2:A9$_2$), but not with the rest of HSFs analyzed in bombarded sunflower leaves, individually or in combination: none (-), LpHSFA2 (A2), hybrid HSF A2:A9$_1$ (A2:A9$_1$).
(G, H, I) BiFC interaction in bombarded sunflower embryos; HaIAA27:YFP^N + HaHSFA4a:YFP^C (G); HaHSFA4a:YFP^N + HaHSFA9:YFP^C (H); HaHSFA4a:YFP^N + HaHSFA9:YFP^C + HaIAA27mIIab (I). Bars 30 µm.
(J) The WT and mutant domain I (mI) HaIAA27 (I27) proteins fully abolished the synergism between HaHSFA4a (A4a) and HaHSFA9 (A9). Analyses performed in bombarded sunflower embryos with the indicated combination of transcription factors.
(K) Active repression assays: a, WT, HaIAA27:GAL4-DB fusion protein (I27), but not the rest of analyzed HaIAA27 fusion proteins (maps on top) efficiently repressed 35S-induced transcription.
Maps of the G4 reporter gene and of the different effectors used in (F) and (H) are shown at the top of the Figure. Numbers in parentheses show the number of replicates for each reporter/effector combination. The same bar shading indicates similar reporter activity. Error bars denote the SE. Asterisks indicate statistically significant synergism.

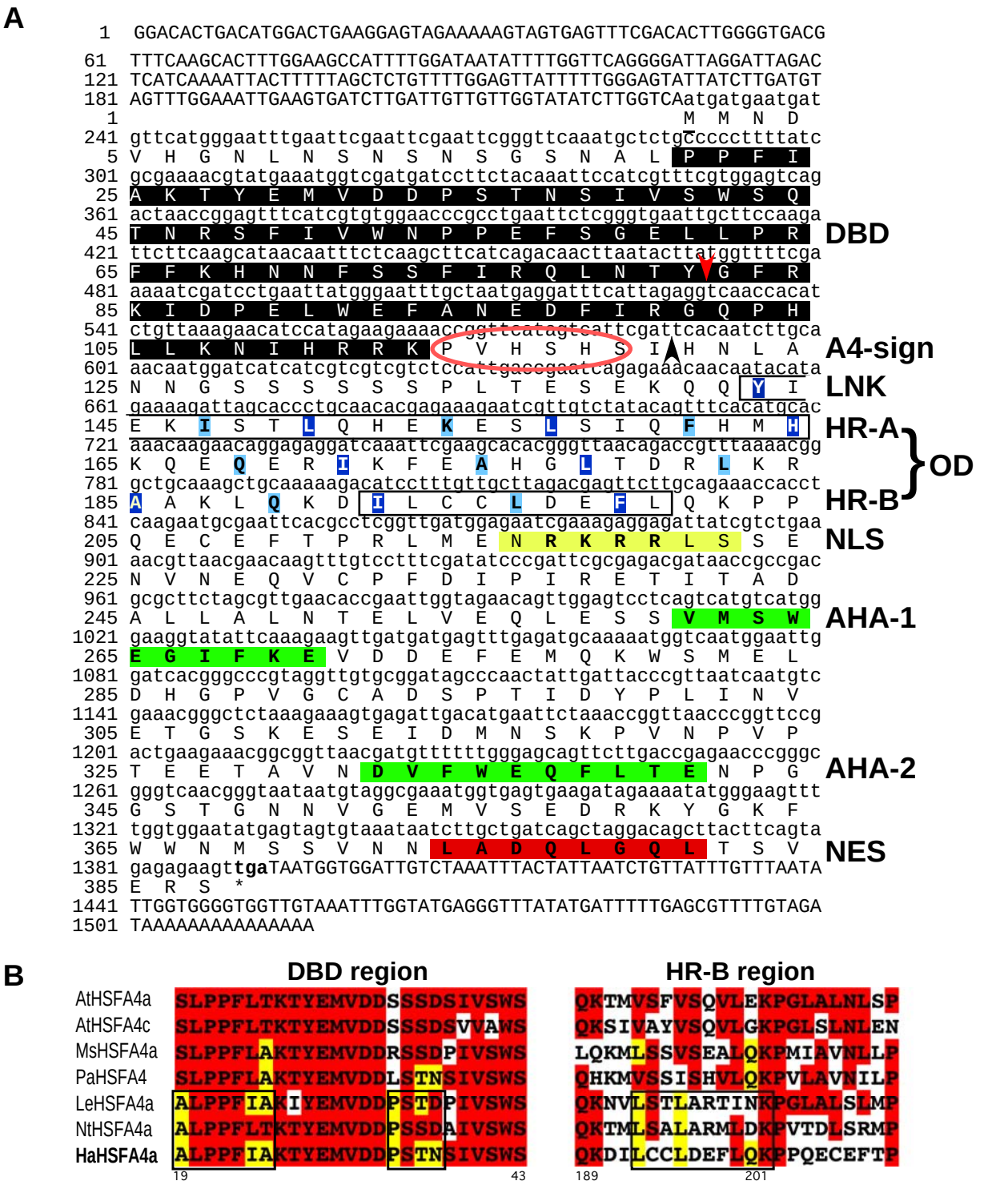

Supplementary Figure S1. **(A)** full-length cDNA sequence and characteristics of the predicted HaHSFA4a protein. Below the nucleotide sequence of HaHSFA4a, we show the predicted amino acid sequence. An asterisk marks the stop codon. The red arrow indicates the expected position for the conserved intron present in the genomic class A HSF sequences. The black arrow marks the 5'-end of the cDNA initially cloned by yeast two-hybrid. To the right, putative domains and functional sequences in the HaHSFA4a protein that were identified based on sequence comparisons with similar HSFs, are indicated. The DNA-binding domain (DBD) is outlined on a black background. Linker (LNK) sequences connect the DBD and the oligomerization domain (OD). These sequences include the HSF Class A4 signature sequences (A4-sign) that are marked with a red oval. The overlapping heptad repeats (HR-A, HR-B, boxed in black) of hydrophobic amino acids that conform the OD are indicated, with the hydrophobic residues outlined on a blue background. The amino acid residues of the putative nuclear localization sequences (NLS) and nuclear export sequences (NES) are outlined on yellow or red backgrounds, respectively. The two putative AHA motifs are indicated on a green background. **(B)** Partial sequence alignment of HaHSFA4a with other Class A4 HSFs. Boxes show amino acid residues (marked in yellow) conserved in HSFs of plants closely related to sunflower.

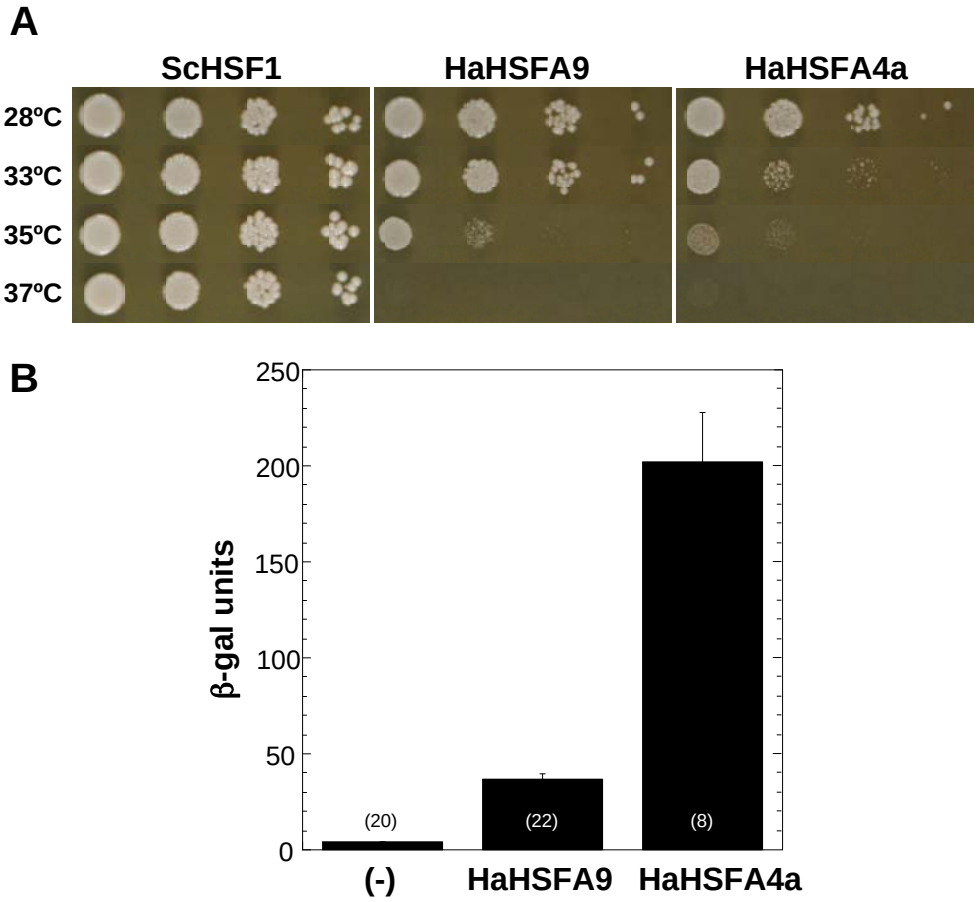

Supplementary Figure S2. HaHSFA4a functions in yeast cells. **(A)** similar functional replacement of the yeast (*Saccharomyces cerevisiae*) ScHSF1 by HaHSFA9 or HaHSFA4a. The sunflower HSFs were cloned in plasmid pADD5 and assayed essentially as described (Almoguera et al., 2002). Aliquots (2.5µl) of the indicated RSY4 yeast strain were spotted on YPD, starting from mid-logphase cultures, at decreasing cell density (1:10 dilutions steps, from left to right). Plates were incubated at the temperatures shown on the left and photographed after 2 days of growth. **(B)** Transcriptional activation assays in yeast using ß-galactosidase reporter plasmids containing the Gal7p promoter in the strain PJ69-4A. The sunflower HSFs were fused to the GAL4DB in pGBT9-derived plasmids. Numbers in parentheses show the number of replicates for each strain/HSF combination.

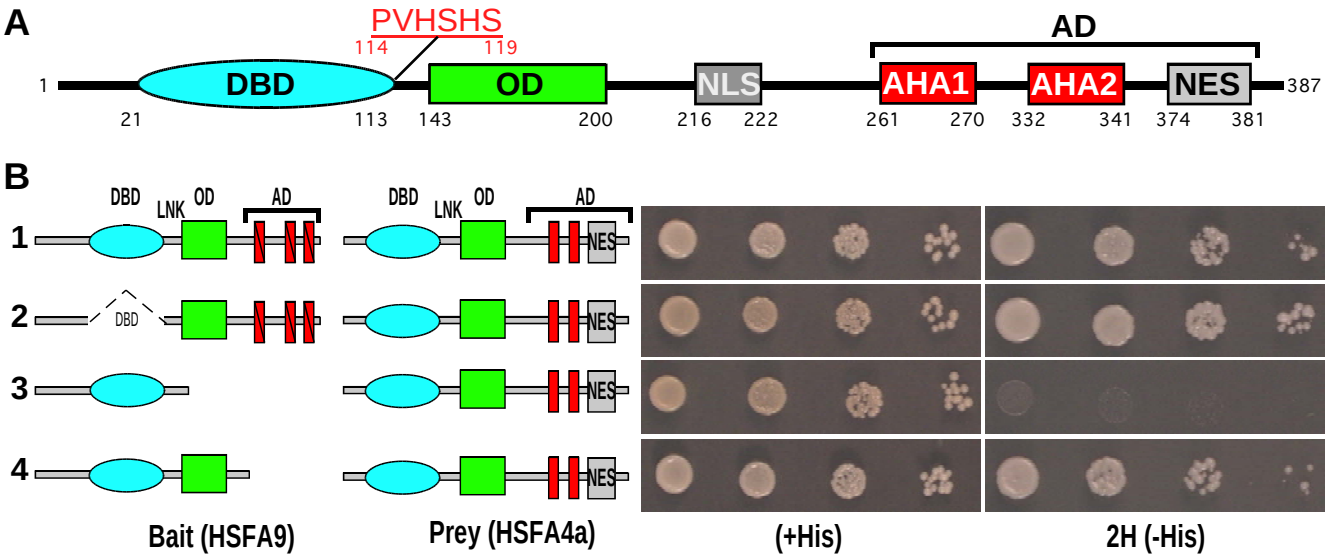

Supplementary Figure S3. Yeast two-hybrid interaction between HaHSFA4a and HaHSFA9. **(A)** Protein domains in HaHSFA4a: the DNA-binding (DBD), oligomerization (OD) and C-terminal activation (AD) domains are indicated. We also show the positions of nuclear localization (NLS) and nuclear export (NES) sequences, as well as that of the two putative AHA motifs (AHA1, AHA2) within the AD. The Class A4 signature sequences (PVHSHS) are depicted. **(B)** Yeast two-hybrid interaction. Aliquots of yeast strains with the indicated "Bait", HSFA9, and "Prey", HSFA4a, plasmids were spotted at decreasing cell density (1:10 dilution steps, from left to right). Interactions were confirmed by observing yeast growth on selective media [2H (-His)], compared with growth on media without selection (+His).The "Bait" plasmids: 1. - HaHSFA9mutAD; 2. - HaHSFA9mutADΔDBD; 3. - HaHSFA9Δ165; 4. - HaHSFA9Δ248.

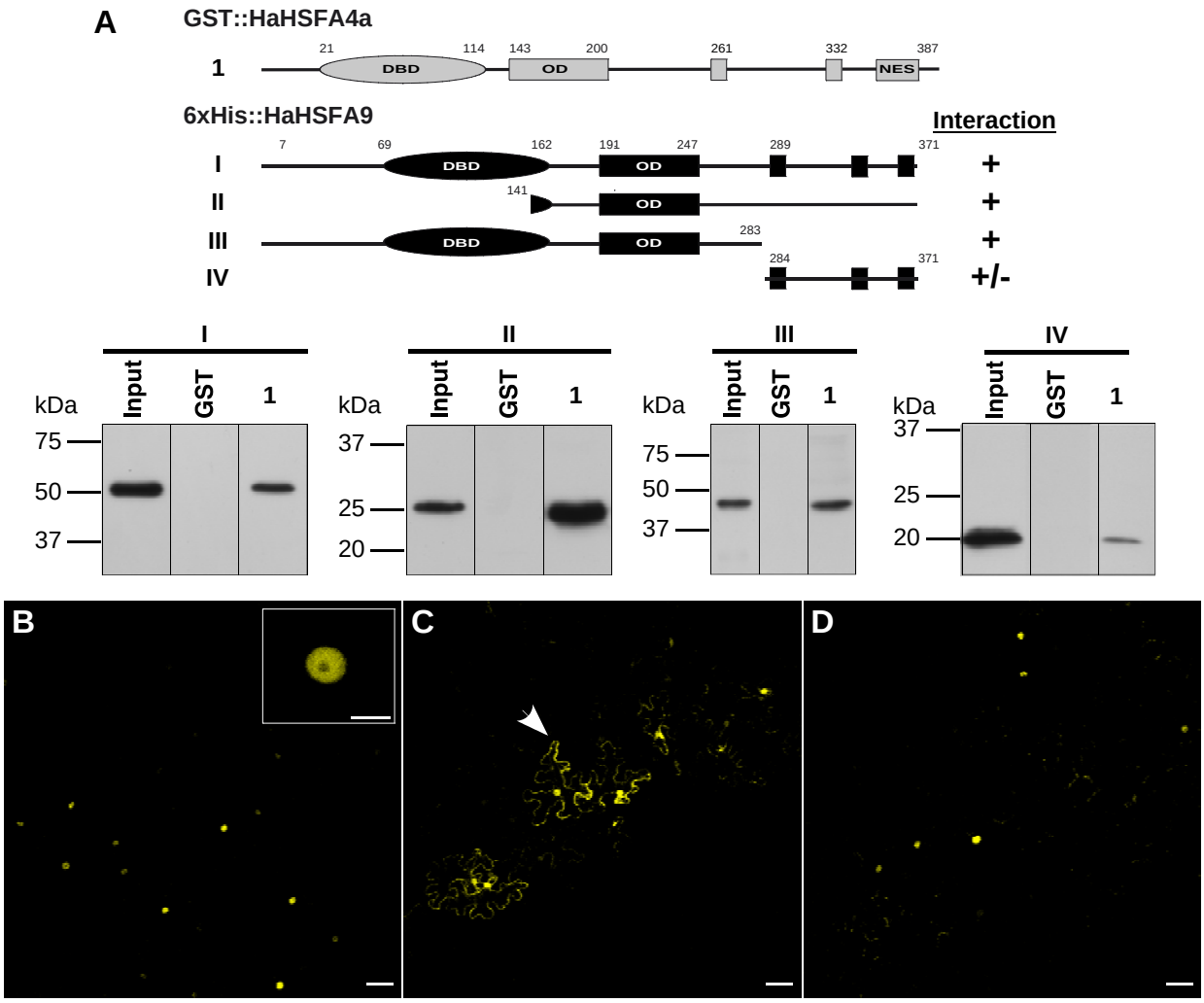

Supplementary Figure S4. *In vitro* and *in planta* interaction between HaHSFA9 and HaHSFA4a. **(A)** *In vitro* GST pull-down interaction. GST and the GST:HaHSFA4a fusion protein (1) were bound to glutathione affinity beads. Beads were incubated with different 6xHis:HaHSFA9 fusion proteins (I-IV). Bottom, the interacting proteins were eluted, and then detected by western blot. **(B to D)** BiFC in leaves of *Nicotiana benthamiana*. Confocal microscopy images of epidermal leaf cells infiltrated with the following fusion proteins: **(B)** HaHSFA9:YFP^{N}+HaHSFA4a:YFP^{C}; the inset shows nuclear fluorescence at higher magnification. **(C)** HaHSFA4a:YFP^{N}+HaHSFA4a:YFP^{C}; the arrow marks fluorescence in a cytosolic band. **(D)** HaHSFA9:YFP^{N}+HaHSFA9:YFP^{C}. Scale bars 50 µm and 12.5 µm (inset).

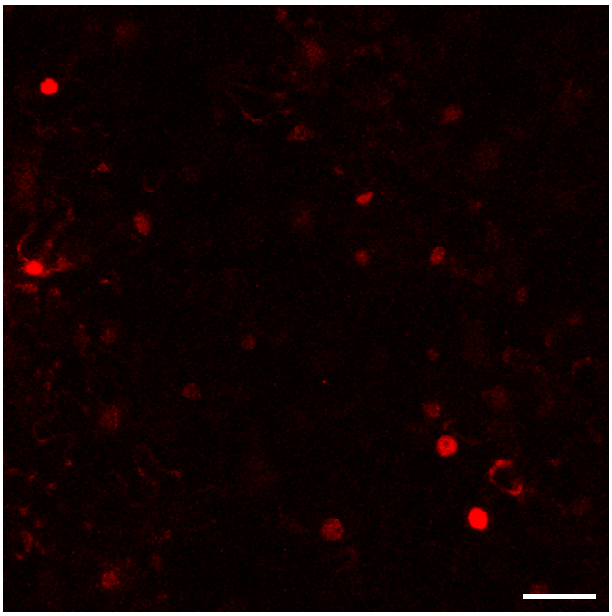

Supplementary Figure S5. Nuclear localization of HaHSFA9 in leaves of *Nicotiana benthamiana*. The leaves were infiltrated with an *Agrobacterium* strain that expressed the fluorescent fusion protein DsRed2:HaHSFA9. The fusion protein was assembled in the pSAT6-DsRed2-C1 plasmid and then transferred to pRCS2 (Tzfira et al., 2005). A confocal laser-scanning Olympus FV1000 microscope, with a UPLSAPO 20x NA:0.75 objective, was employed using standard DsRed2 filter settings for image acquisition. Scale bar, 50 μm.

	luc/Rluc±SE		
TF combination	**Co-bomb**	**Sum**	**ANOVA**
A9+A4a [Fig. 1F]	49.14±2.86	24.42±0.66	F=100.2, **P=0.0001**
A2:A9$_2$+A4a [Fig. 1F]	30.22±2.94	21.65±1.56	F=6.273, **P=0.013**
A2:A9$_1$+A4a [Fig. 1F]	21.88±1.50	18.79±1.29	F=0.682, P=0.410
A2+A4a [Fig. 1F]	20.68±1.75	20.08±0.99	F=0.026, P=0.871
A9+A4a [Fig. 1J]	615.7±49.7	309.8±18.1	F=30.62, **P=0.0001**

Supplementary Table S1. Statistical analysis of the synergistic interactions observed by transient expression in sunflower. Data from the indicated TF combinations and Figures were analyzed following the logarithmic normalization and one-way ANOVA procedures previously described (Almoguera et al., 1998; Rojas et al., 2002). When indicated, we show the SE and mean reporter activity (luc/Rluc) obtained after co-bombardment (Co-bomb) and from the sums of the activities separately induced by the corresponding TFs. Note that from each sum of two individual activity values, the basal level (activity without TF) was subtracted once. The statistic (F) and probability (P) values are shown for each comparison between the Co-bom and Sum mean activities. Statistically significant differences (P< 0.05) are indicated with bold face.

METHODS

Cloning of the full-length HaHSFA4a cDNA

The complete HaHSFA4a cDNA sequences were assembled in plasmid pUC-HaHSFA4a from two DNA fragments of 921 bp and 610 bp. The first fragment contained the coding sequence of HaHSFA4a downstream of the *BsaB*I site (position 608) and the 3'-UTR to position 1516. This fragment was derived, by digestion with *BsaB*I and *Bgl*II, from one of the plasmids with a clone obtained by two-hybrid screening of the sunflower embryo cDNA library (Almoguera et al., 2002), pGAD424#33. The rest of coding sequences and the 5'-UTR sequences of HaHSFA4a were obtained by RNA Ligase-mediated amplification (RLM-RACE, see Almoguera et al., 2002). For RLM-RACE, we used an oligonucleotide specific for HaHSFA4a. This HSFA4-RACE primer (5'-GGAGACGACGACGATGATGATCCATT-3') spans from positions 629 to 604 in the non-coding strand. The PCR-amplified sequences were cloned in plasmid pCR^{R}4-TOPO^{R} (Invitrogene). We obtained plasmid pCR^{R}4-TOPO^{R} -HaHSFA4a-5'#35, which was used to obtain the 610 bp fragment by PCR amplification followed by *Xba*I digestion. The amplification was with 5'-aaacgaattcgcctctaGACACTGACATGGACTGA-3', which contains a *Xba*I site placed next to position 1 of HaHSFA4a, and with 5'-TGATCCATTGTTTGCAAGATT-3', starting with the *BsaB*I half-site at position 612; both sites are respectively underlined. The 921 bp and 610 bp fragments were combined by their ligation between the *Xba*I and *BamH*I sites of the pUC19 vector, which originated pUC-HaHSFA4a. The sequence of the two strands of the HaHSFA4a cDNA in pGAD424#33 plasmid (positions 588-1716) and those of all PCR-amplified fragments was obtained and verified. The same applies for the rest of PCR-amplified sequences for the rest of plasmid constructs in this report.

Two-hybrid cloning and interaction assays is yeast

Conditions for cDNA library (Almoguera et al., 2002) screening, and for the interaction assays were essentially as described (Carranco et al., 2010). The positive clones obtained were verified, after retransformation in the PJ69-

4A yeast strain (James et al., 1996), by their ability to grow in selective medium without leucine, tryptophan and histidine, supplemented with 50 mM 3-AT. The pGBT9-derived HaHSFA9 plasmids numbered 1 and 2 in Supplementary Figure S3B have been previously described, respectively as pGBT9-HaHSFA9mAD and pGBT9-HaHSFA9ΔDBD (Carranco et al., 2010). pGBT9-HaHSFA9Δ166 (numbered 3 in Supplementary Figure S3B) contains a PCR-amplified fragment of 533 bp, with amino-acid residues 1 to 166 from HaHSFA9 inserted in frame at the *Sma*I site of pGBT9. pGBT9-HaHSFA9Δ284 (numbered 4 in Supplementary Figure S3B) was constructed by a similar insertion at this site of a 867 bp fragment with amino-acid residues 1 to 283 from HaHSFA9. The HaHSFA4a prey plasmid, pGAD424-HaHSFA4a, contains the complete coding sequence of HaHSFA4a (amino acids 1-387) cloned in frame between the *Nco*I and *Pst*I sites of the pGAD424 vector (Clontech). The required restriction sites, at the ends of the PCR-amplified fragment of 1333 bp, were introduced with the oligonucleotides 5'-GGTATATCTTGGTCcATGgTGAATGATGTTCATGGGAATTTG-3' and 5'-GAGCTCGGTACCCGGGGATCTGCAG-3'. The respective sites are underlined.

GST pull-down

The complete HaHSFA4a coding sequence (Supplementary Figure S1A) was fused in frame with GST (construct 1, Supplementary Figure S4A) at the *Sma*I site of plasmid pGEX4t-1 (Amersham Biosciences). The 6xHis-tagged versions of the HaHSFA9 proteins, I to IV, used for the experiments of Supplementary Figure S4A have been previously described (Díaz-Martín et al., 2005). Recombinant protein expression in bacteria, *in vitro* pull-down and western blot detection of the interacting proteins was essentially as described (Díaz-Martín et al., 2005).

***In planta* BiFC interaction and protein localization assays**

For the assays in leaves of *Nicotiana benthamiana*, 3 to 4 week-old plants were grown and infiltrated with mixtures of *Agrobacterium* strains, which

contained the required plasmid combinations, as described (Carranco et al., 2010). 48 h after infiltration, disc sections from the infiltrated leaves were analyzed.

For the protein localization assays of Figure 1A-E, the infiltrated leaf sections were analyzed with a confocal laser-scanning Olympus FV1000 microscope. In this case we used UPLSAPO 20x NA:0.75 objective and standard GFP filter settings. Image analysis was performed with FV10-ASW 1.7 and Adobe Photoshop 7.0 software. Image acquisition conditions were adjusted for each sample, to avoid saturation in most of the pictured area. GFP-fusion constructs: The, PCR-amplified, coding region of HaHSFA4a was inserted between the *Sal*I and *Sma*I sites of the pSAT6-EGFP-C1 plasmid (Tzfira et al., 2005). The HaHSFA4a:GFP fusions were transferred from the pSAT6-EGFP-C1 plasmid to the pRCS2-*nptII* binary vector (Tzfira et al., 2005), and used in *N. benthamiana*. The WT and NESmut HaHSFA4a fusions differ in six nucleotide substitutions, which were introduced by a, two-step, megaprimer PCR-mutagenesis (see Chen and Przybyla, 1994; Carranco et al., 2010). We used the pSAT6-EGFP:HaHSFA4a plasmid as the amplification template and 5'-TGTAAATAATgcTGCTGATCAGgcAGGACAGgcTACTTCAGTAGAGAGA-3' as the mutagenic primer. This resulted in three amino acid substitutions at positions 374, 378 and 381 (of leucine by alanine).

In the experiments of Figure 1C-E, the strain with the HaHSFA4a:GFP fusion was also co-infiltrated with strains containing non-fluorescent YFP^C fused to HaHSFA9, or to the $A2:A9_1$ and $A2:A9_2$ hybrid proteins. The $A9:YFP^C$ fusion (Carranco et al., 2010) and the $A2:A9_1$ hybrid protein (HSFA2-A9C in Díaz-Martín et al., 2005) have been previously described. Construction of the $A2:A9_2$ hybrid protein is described below.

For the experiments in Supplementary Figure S4B-D, BiFC was studied under a Leica TCS-SP2 confocal laser-scanning microscope with a HC PL FLUOTAR 20x/0.50 objective. We used standard YFP excitation and detection settings. Image analysis was carried out with Leica LCS software and Adobe Photoshop 7.0. For BiFC assays in sunflower embryos (Figure 1G-I), 15 dpa embryos were bombarded and analyzed using the Olympus FV1000

microscope as described (Carranco et al., 2010). Plasmid constructs for BiFC in embryos were derived from the SPYCE(M) and SPYNE173 vectors (Waadt et al., 2008). The HaHSFA9, HaHSFA4a, and hybrid-HSF sequences fused to the non-fluorescent YFP-halves in these constructs were PCR-amplified from the respective effector plasmids used for the transient activation assays (see below). The interference of HaIAA27 on the BiFC between HaHSFA4a and HaHSFA9 in embryos (see Figure 1H-I) was analyzed by cobombardment of 5 µg of a plasmid encoding the HaIAA27 stabilized mutant mIIab (pBI221-HaIAA27mIIab, see Carranco et al., 2010). The same amount of pBI221 plasmid was used as a negative control. For BiFC and protein localization in leaves, we used the SPYCE (YFP^C) and SPYNE (YFP^N) fusions transferred to the corresponding binary vectors: kanII-SPYCE(M) and kanII- SPYNE173 (Waadt et al., 2008).

Transient activation and repression assays in sunflower

For the assays of Figure 1J and 1K, 15 dpa sunflower embryos were used to insure that the WT form of HaIAA27 is stabilized (Carranco et al., 2010). Bombardment was as in (Díaz-Martín et al., 2005), except for the reporter plasmid used [-1132(G4):LUC] and for the amounts of pBI221-HaHSFA9 and pBI221-HaIAA27 effectors (40 ng and 5 µg, respectively). The total amount of plasmid DNA was adjusted with pBI221 to 13.5 µg. For the assays in Figure 1F, bombardment of sunflower leaves was performed essentially as described (Tejedor-Cano et al., 2010). The amounts of plasmid DNA were as in Figure 1J except for the amounts of effector plasmids: 125 ng of pRT-LpHSFA2 (Rojas et al., 2002), and 20 ng of pBI221-HaHSFA9, pRT-A2:$A9_1$ or pRT-A2:$A9_2$. The total amount of plasmid DNA was adjusted with pBI221 to 8.5 µg. Mean *Photinus* luciferase (luc) activity was normalized with *Renilla* luciferase (Rluc).

We have previously described the internal reference plasmid (pBI221-Rluc; Díaz-Martín et al., 2005) and most of the reporter and effector plasmids used for transient assays and as a source for the fusion proteins employed in this report: (G4), -1132(G4):LUC (Tejedor-Cano et al., 2010), pBI221-HaHSFA9 (Almoguera et al., 2002), pBI221-HaIAA27 (Carranco et al., 2010), pRT-

LpHSFA2 (Rojas et al., 2002), and pRT-A2:A9$_1$ (pRT-HSFA2-A9C in Díaz-Martín et al., 2005). The HaHSFA4a effector plasmid, pBI221-HaHSFA4a, was constructed from pUC-HaHSFA4a. The 1514 bp fragment (containing 228 bp of 5'-UTR, 1163 bp of coding sequences, and 123 bp of 5'-UTR) obtained by digestion of pUC-HaHSFA4a with *Xba*I and *Sac*I was introduced between these restriction sites in pBI221 (Acc AF502128). The A2:A9$_2$ hybrid HSF contains the LpHSFA2 sequences from amino acids 1 to 136, followed by HaHSFA9 sequences from amino acids 164 to 371. The A2:A9$_2$ protein was obtained by PCR-based fusion (Hobert, 2002; Díaz-Martín et al., 2005). PCR1 (with an annealing temperature of 57ºC) was performed with the oligonucleotides 5´-ACTATCCTTCGCAAGACCCTTCC-3' (OliA, Díaz-Martín et al., 2005) and 5´-gtttttgtgtgttttgtggctgGCAAGCACCAGATCCTTGTTGATT-3' (OliB), using pRT-LpHSFA2 (Rojas et al., 2002) as the template for amplification. The lowercase sequences in OliB are a 22-nucleotide overhang that encodes HaHSFA9 amino acids from position 164. The uppercase sequences encode LpHSFA2 amino acids ending at position 136. PCR2 (with an annealing temperature of 51ºC) was performed with the oligonucleotides 5'-CAGCCACAAAACACACAAAAAC-3' (OliC) and 5'-TCGGAATTAACCCTCACTAAAG-3', (OliD, T3 sequences), using pSKHSFA9-F (Almoguera et al., 2002) as the amplification template. The OliC sequences are the reverse complement of the 22-nucleotide overhang contained in OliB. The fusion PCR (with an annealing temperature of 47ºC) was performed with OliA and 5'-TCTAGAACTAGTGGATC-3' (OliD'). OliD' contains, nested, SK sequences that are located 59 nucleotides upstream of OliD. We used the mixed, unpurified, products of PCR1 (501 bp) and PCR2 (786 bp) as the amplification template (approximately 10 ng DNA each). The product of fusion PCR (1198 bp) was digested with *Xho*I and *Xba*I. The resulting DNA fragment (1160 bp) was used to replace the *Xho*I-*Xba*I fragment of pRT-LpHSFA2 (1335 bp), thus originating the effector plasmid pRT-A2:A9$_2$. The two effector plasmids that express the domain I-mutant forms of HaIAA27 used in Figure 1J, derive from the previously described pGAD424-HaIAA27 and pBI221-HaIAA27 plasmids (Carranco et al., 2010). We introduced the desired amino acid substitutions with megaprimer PCR using plasmid pGAD424-HaIAA27 as the amplification template (Carranco et al., 2010). The oligonucleotides 5'-

GTGACTCAGAACCAGGcgcACCggcTCTtgcCTCGGTGGCTTTCAAG-3' and 5'-CTCGGTGGCTTTagcGTTagcATCTTGGTTGTGGGTTTTGGG-3' were used, respectively for obtaining the HaIAA27mIa and HaIAA27mIab mutant megaprimers. The HaIAA27mIab megaprimer was obtained by PCR from the HaIAA27mIa plasmid. The PCR-amplified fragments that contain the respective mutant HaIAA27 sequences were cloned in pBI221. We thus obtained the pBI221-HaIAA27mIa and pBI221-HaIAA27mIab effector plasmids. All PCR-amplified fragments were verified by DNA sequencing.

For the active-repression assays of Figure 1K, the 35S-GAL4-TATA-LUC-NOS reporter plasmid (Hiratsu et al., 2004, 35S:5xGAL4:LUC) was bombarded to 15 dpa sunflower embryos together with different effector plasmids. These plasmids express the GAL4 binding domain (GAL4DB,) or different fusion proteins, including that of HaIAA27, the HaIAA27ΔN deletion, and fusions to the domain-I-mutant proteins used for the experiments of Figure 1J. The amounts of plasmid DNA per precipitate (5 shots) were: 2.5 µg of the reference plasmid, 5 µg of the reporter plasmid and 5 µg of the effector plasmids. The effector plasmids derive from pBI524-GAL4DB (Després et al., 2003).

Statistical analyses

Differences between the reporter gene activities observed in transient expression were tested using ANOVA. Statistical analyses have been previously described in depth (Prieto-Dapena et al*.,* 2006 and 2008).

References

Almoguera, C., Rojas, A., Díaz-Martín, J., Prieto-Dapena, P., Carranco, R., and Jordano, J. (2002). A seed-specific heat-shock transcription factor involved in developmental regulation during embryogenesis in sunflower. J. Biol. Chem. **277,** 43866-43872.

Chen, B., and Przybyla, A.E. (1994). An efficient site-directed mutagenesis method based on PCR. Biotechniques **17,** 657-659.

Després, C., Chubak, C., Rochon, A., Clark, R., Bethune, T., Desveaux, D., Fobert, P.R. (2003). The Arabidopsis NPR1 disease resistance protein is a novel cofactor that confers redox regulation of DNA binding activity to the basic domain/leucine zipper transcription factor TGA1. Plant Cell **15,** 2181-2191.

Díaz-Martín, J., Almoguera, C., Prieto-Dapena, P., Espinosa, J.M., and Jordano, J. (2005). Functional interaction between two transcription factors involved in the developmental regulation of a small heat stress protein gene promoter. Plant Physiol. **139,** 1483-1494.

Hiratsu, K., Mitsuda, N., Matsui, K., and Ohme-Takagi, M. (2004). Identification of the minimal repression domain of SUPERMAN shows that the DLELRL hexapeptide is both necessary and sufficient for repression of transcription in Arabidopsis. Biochem. Biophys. Res. Commun. **321,** 172-178.

Hobert, O. (2002). PCR fusion-based approach to create reporter gene constructs for expression analysis in transgenic C. elegans. Biotechniques **32,** 728-730.

James, P., Halladay, J., and Craig, E.A. (1996). Genomic libraries and a host strain designed for highly efficient two-hybrid selection in yeast. Genetics. **144,** 1425-1436.

Prieto-Dapena, P., Castaño, R., Almoguera, C., and Jordano J. (2008). The ectopic overexpression of a seed-specific transcription factor, HaHSFA9, confers tolerance to severe dehydration in vegetative organs. Plant J. **54,** 1004-1014**.**

Rojas, A., Almoguera, C., Carranco, R., Scharf, K.D., and Jordano J. (2002). Selective activation of the developmentally regulated *Hahsp17.6 G1* promoter by heat stress transcription factors. Plant Physiol. **129,** 1207-1215.

Tzfira, T., Tian, G.W., Lacroix, B., Vyas, S., Li, J., Leitner-Dagan, Y., Krichevsky, A., Taylor, T., Vainstein, A., Citovsky, V. (2005). pSAT vectors:

a modular series of plasmids for autofluorescent protein tagging and expression of multiple genes in plants. Plant. Mol. Biol. **57,** 503-516.

Waadt, R., Schmidt**, L.K., Lohse, M., Hashimoto, K., Bock, R., Kudla, J.** (2008). Multicolor bimolecular fluorescence complementation reveals simultaneous formation of alternative CBL/CIPK complexes in planta. Plant J. **56,** 505-516.